Science of the Total Environment 786 (2021) 147515

Contents lists available at ScienceDirect

Science of the Total Environment

journal homepage: www.elsevier.com/locate/scitotenv

Activity and structure of methanogenic microbial communities in sediments of cascade hydropower reservoirs, Southwest China

Debin Wu [a,b], Yuan Zhao [a,b], Lei Cheng [c], Zhuo Zhou [c], Qiusheng Wu [a], Qian Wang [a,b], Quan Yuan [a,*]

[a] State Key Laboratory of Environmental Geochemistry, Institute of Geochemistry, Chinese Academy of Sciences, Guiyang 550081, China
[b] University of Chinese Academy of Sciences, Beijing 100049, China
[c] Key Laboratory of Development and Application of Rural Renewable Energy, Biogas Institute of Ministry of Agriculture, Chengdu 610041, China

HIGHLIGHTS

- Methylotrophic methanogenesis could be important in reservoir sediments.
- Terrestrial OM largely stimulates CH_4 production despite recalcitrant to decomposition.
- HRT controls activity and structure of methanogenic community of reservoir sediments.

GRAPHICAL ABSTRACT

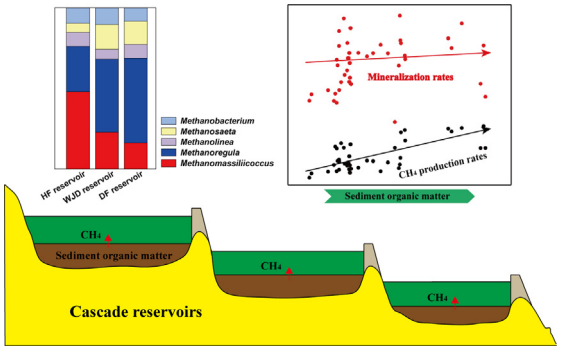

ARTICLE INFO

Article history:
Received 15 January 2021
Received in revised form 29 April 2021
Accepted 30 April 2021
Available online 4 May 2021

Editor: Ashantha Goonetilleke

Keywords:
Reservoirs
Sediment organic carbon
Methane production
Archaea
Metagenomic sequencing

ABSTRACT

Freshwater reservoirs are an important source of the greenhouse gas methane (CH_4). However, little is known about the activity and structure of microbial communities involved in methanogenic decomposition of sediment organic matter (SOM) in cascade hydropower reservoirs. In this study, we targeted on sediments of three cascade reservoirs in Wujiang River, Southwest China. Our results showed that the content of sediment organic carbon (SOC) was between 3% and 11%, and it's positively correlated with both C/N ratio and recalcitrant organic carbon content of SOM. Meanwhile, SOC content was positively correlated with CH_4 production rates but had no significant correlation with total CO_2 production rates of the sediments, when rates were normalized to sediment volume. Resultantly, the sediment anaerobic decomposition rates hardly significantly increase along with the SOC content. These results suggested that the terrestrial organic matter accumulated after damming stimulated CH_4 production from the reservoir sediments even though its decomposition rate was limited. Meantime, high throughput sequencing of 16S rRNA genes indicated that not only the hydrogenotrophic and acetoclastic, but also the methylotrophic methanogens (*Methanomassiliicoccus*) are abundant in the reservoir sediments. Moreover, metagenomic sequencing also suggested that methylotrophic methanogenesis are potentially important in the sediment of cascade reservoirs. Finally, the hydraulic residence time of the reservoir could be the key controlling factor of the structures of bacterial and archaeal communities as well as the CH_4 production rates of the reservoir sediments.

1. Introduction

Methane (CH_4) is the second most important greenhouse gas next to CO_2, the global CH_4 emissions are about 500–600 Tg C y^{-1} (Conrad,

* Corresponding author.
E-mail address: yuanquan@mail.gyig.ac.cn (Q. Yuan).

https://doi.org/10.1016/j.scitotenv.2021.147515
0048-9697/

2009; Saunois et al., 2020). Freshwater ecosystems are an important source of CH_4 to the atmosphere (about 122–159 Tg C y^{-1}) (Deemer et al., 2016; Saunois et al., 2016). Among them, the global CH_4 emissions from hydroelectric reservoirs are about 4.4–18.4 Tg C y^{-1} (Barros et al., 2011; Li and Zhang, 2014). In freshwater ecosystems, anaerobic sediments are hotspots for microbial methanogenesis during anaerobic mineralization (Bastviken et al., 2008; Gruca-Rokosz and Tomaszek, 2015; Sepulveda-Jauregui et al., 2018). Anaerobic microbial degradation of organic matter, which produces both CH_4 and CO_2 as the end products, are accomplished consecutively by a complex microbial community consisting of hydrolytic, fermentative, syntrophic, homoacetogenic bacteria and methanogenic archaea (Conrad, 1999).

Based on the substrates used to produce methane, methanogenesis can be achieved by utilizing hydrogen (H_2) plus carbon dioxide (CO_2) (hydrogenotrophic pathway), acetate (acetoclastic pathway) and methyl compounds (methylotrophic pathway) (Thauer et al., 2008). In most anoxic environments, CH_4 is produced from either acetoclastic methanogenesis or hydrogenotrophic methanogenesis (Whiticar et al., 1986; Falz et al., 1999; Conrad et al., 2007; Conrad, 2020). In contrast, methylotrophic methanogenesis was reported to be important in saline and marine environments (Nobu et al., 2016; Zhuang et al., 2016; Evans et al., 2019; Zhang et al., 2020) but seldom found in freshwater ecosystems. For example, in the sediment of freshwater ecosystems, the major methanogenic pathways are thought to be hydrogenotrophic and acetoclastic pathways (Falz et al., 1999; Borrel et al., 2011; Conrad, 2020), and their dominant methanogen groups usually belong to genera *Methanoregula*, *Methanolinea*, *Methanobacterium*, and *Methanosaeta* (Biderre-Petit et al., 2011; Borrel et al., 2011; Youngblut et al., 2014; Berberich et al., 2020). But most of them investigated the composition of methanogenic communities in sediment of freshwater lakes but rarely in reservoirs.

In an effort to alleviate the growing water shortages and energy demands, numerous hydroelectric dams have been constructed worldwide (Maavara et al., 2015). Damming the river would lead to hydrological status variations, silt deposition, nutrients blocking and so on (Wang et al., 2011; Chen et al., 2019). For instance, damming has attenuated by 26% the transport of terrestrial organic matter to the ocean (Dean and Gorham, 1998; Syvitski et al., 2005). Compared with freshwater lakes, reservoirs tend to have higher watershed area-to-surface area ratio that could result in richer organic matter input from the surrounding catchment (Hayes et al., 2017), and this could lead to higher C burial rates in the reservoirs (Knoll et al., 2014). All of the effects are conducive to the continuous accumulation of sediment organic matters (SOM) which might strongly stimulate methane production in the reservoirs.

China has constructed more than 90,000 reservoirs with a total water storage capacity over 8.1×10^{11} m^3, ranking first in the world for the number of reservoirs (Lehner et al., 2011; Wang et al., 2018a; Chen et al., 2019). Many of these reservoirs are built in a cascade configuration in large rivers of Southwest China. Previous studies have reported active CH_4 emissions from the cascade reservoirs (Zheng et al., 2011; Shi et al., 2017; Liu et al., 2020), and CH_4 flux were often largely different among the cascade reservoirs located in the same river (Barros et al., 2011; Shi et al., 2017; Liu et al., 2020). However, the characteristics of methanogenic decomposition of SOM, as well as structure of methanogenic communities in sediments of cascade reservoirs are largely unclear. We hypothesized that the different hydraulic residence times probably lead to distinct methanogenic potentials and methanogenic microbial communities of the sediments among the cascade reservoirs.

In this study, three cascade reservoirs of Wujiang River, which is located in Southwest China and one of the earliest cascade hydroelectric development rivers in China, were chosen to study the activity and structure of microbial communities involved in methanogenic decomposition of SOM in sediments. The objectives of this study were to: (1) evaluate the CH_4 and CO_2 production rates during anaerobic decomposition of SOM in cascade reservoirs, (2) analyse the structure of methanogenic microbial communities in sediments of cascade reservoirs, (3) explore the main biogeochemical parameters affecting methanogenic decomposition of SOM as well as composition of bacterial and archaeal communities.

2. Methods

2.1. Description of study area

The Wujiang River (26°07′–30°22′N, 104°18′–109°22′E) is the largest tributary on the right bank of the upper reaches of the Yangtze River. It has a total length of 1037 km with a fall of 2124 m. The Wujiang River mainly flows through the typical karst area of Southwest China. It has an annual runoff of 53.4 billion cubic meters, and its annual average rainfall (1195 mm) occurred mostly in spring and summer. A series of hydropower reservoirs have been constructed along the Wujiang River. Three reservoirs, Hongfeng (HF), Wujiangdu (WJD) and Dongfeng (DF) were selected for this study. The HF reservoir is the first and most upstream reservoir in a major tributary of the Wujiang River, the other two reservoirs are located on the middle reaches of the Wujiang River (Wang et al., 2013). The main features of these reservoirs are described in Table S1. In these reservoirs, the temperature, DO, pH and Chl a of the surface water were about 10.4 °C–28.2 °C, 6.1 mg/L–13.6 mg/L, 7.7–8.8 and 5.8 μg/L–25.2 μg/L, respectively (Xiao et al., 2021). These reservoirs showed thermal stratification mainly in summer, and the thermocline appeared at a layer of around 5–20 m depths (Wang et al., 2020a; Wang et al., 2020b; Xiao et al., 2021). Meantime, these reservoirs exhibit various hydrographic characteristics and nutrient levels, and the HF reservoir has higher trophic levels than the others (Xiao et al., 2021). Temperature of the bottom water of these reservoirs is around 15 °C in at least half of the year and the maximum is around 22 °C (Chen et al., 2019; Wang et al., 2019).

2.2. Sediment sampling

The DF and WJD reservoirs are canyon type reservoirs. So the sediment cores usually could only be collected at relatively central area where the sediment is mainly accumulated at. In contrast, the HF reservoir is located in karst plateau and its surface area is about three times of the other two reservoirs (Table S1). Therefore, we prepared much more sampling sites in HF reservoir. From June to August 2018, sediment samples (three replicates per sampling site) were collected in these cascade reservoirs. 9 sampling sites were prepared for HF (named H1-H9), 3 sampling sites for DF (D1, D2, D3) and 2 sampling sites for WJD (W1, W2) reservoirs. In April 2019, another sediment sample in HF (named HS) was collected nearby samples of H1 and H6 for metagenomic sequencing. Detailed information of sampling sites are listed in Fig. 1 and Table S2. Sediment cores were taken in triplets in each site using a gravity corer (internal diameter 5.9 cm). Sediment cores were sealed from both ends and transported vertically to the laboratory within 12 h. Then the sediment cores were kept in dark at 15 °C until use within 3 days.

2.3. Incubation of sediment samples

For incubation experiment, the 2–15 cm depth of sediment cores of each sampling site was collected and homogenized, and 20 g sediment sample was added into 100 ml glass vial for anaerobic incubation, then 3 ml filtered overlying water was added into each vial. The whole process was made oxygen free by continuous flushing with pure nitrogen. Then the vials were sealed immediately with butyl rubber stopper together with aluminum crimp. After repeatedly vacuumed and flushed with pure N_2 for 3 min, the vials were incubated statically at 15 °C and 25 °C under dark condition for four days. Three replicates were prepared for each sediment sample. A small part of the remaining sample was

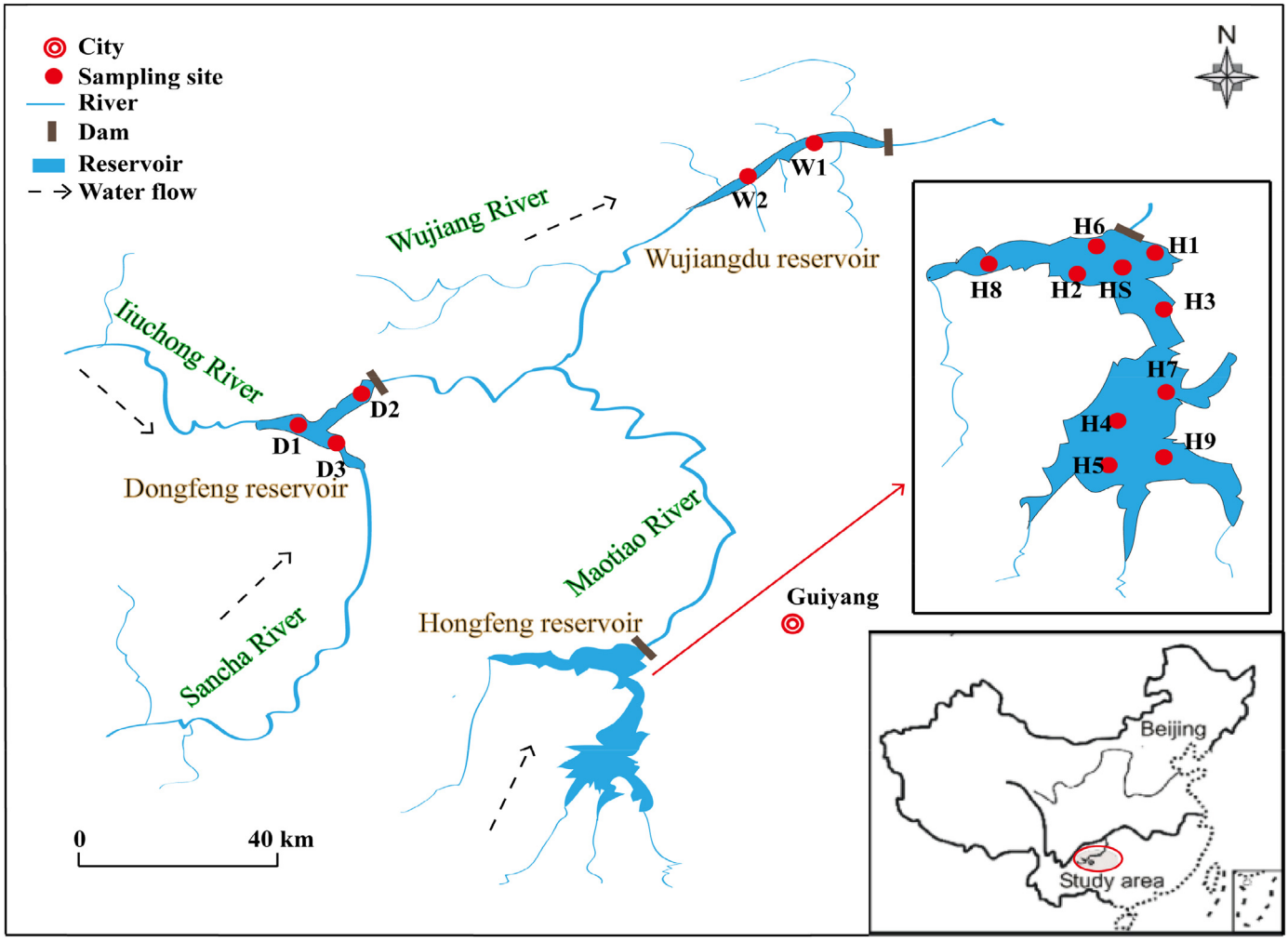

Fig. 1. Geographical location and distribution of sampling sites in three (Hongfeng, Wujiangdu and Dongfeng) reservoirs of Wujiang River basin, which is located in Guizhou Province, China. The brown bars denote dams, black dotted arrows indicate the flow direction of river water, the red dots denote sampling sites.

centrifuged and stored at −20 °C for subsequent analysis of sediment and porewater samples.

2.4. Measurement of CH_4 and CO_2 production

At the end of the incubation (day 4), gas samples (300 μl) from the headspace of vials used for sediment anaerobic incubation were taken with a gas-tight pressure lock syringe (VICI, Baton Rouge, USA), after the vials were vigorously shaken by hand, and injected immediately into gas chromatograph (HP6890, Hewlett Packard Co., USA) equipped with flame ionization detector (FID), so as to analyse the concentrations of CH_4 and CO_2. The CO_2 was measured after conversion to CH_4 with a methanizer (nickel catalyst at 375 °C). Then the vials were opened and pH values of the sediment samples were measured so as to calculate the bicarbonate CO_2 in the vials.

Total CO_2 was defined as the sum of gaseous, dissolved and bicarbonate CO_2. The amounts of CO_2 and CH_4 gases in the headspace of the vials were calculated based on the partial pressures using the volume of the gas space and the gas constant. The amounts of dissolved and bicarbonate CO_2 in the liquid were calculated as described in Yuan et al. (2018). The mineralization rates of sediment organic matter were calculated from the accumulation of total CO_2 plus CH_4 production during the incubation (Moodley et al., 2005; Yuan et al., 2018). Similarly, the production rates of CH_4 and total CO_2 were calculated from the accumulation of CH_4 and total CO_2 during the incubation, respectively. All the production rates described above were expressed normalized to both sediment volume (μmol cm^{-3} d^{-1}) and mass of sediment organic carbon (μmol g SOC^{-1} d^{-1}). So as to know the actual volume of the sediment in each vial, the bulk density of the sediment samples was determined (ranged from 1.02 g/ml ~1.27 g/ml). The mass of SOC per vial was calculated from the water content of the sediment samples and the SOC content of the dried sediment samples.

2.5. Analysis of sediment biogeochemical parameters

After acidification and lyophilization, the contents of sediment organic carbon (SOC), total sulfur (TS) and total nitrogen (TN) of the sediment samples were analyzed with elemental analyzer (Vairo Macro CNS, Elementar, Germany). For Fe (II) and Fe (III) determination, sediment samples (0.5 g) were extracted with 4.5 ml of 0.5 M HCl at room temperature for 24 h. Then 100 μl of the HCl suspension was added to 1 ml Ferrozin solution (0.1% w/w Ferrozin in 50 mM N-2-hydroxylethylpiperazin-N′-2-ethane sulfonate, pH 7), mixed and centrifuged at 8000 rpm for 5 min. The supernatant was measured with a photometer at 562 nm. Total free iron (Fe (II) + Fe (III)) was determined by adding 100 μl of the HCl suspension to 2 ml 0.25 M hydroxylamine hydrochloride in 0.25 N HCl followed by incubation at 60 °C for 2 h and then analyzing Fe (II) as described above (Schnell et al., 1998).

The infrared spectrum of sediment organic matter (SOM) was analyzed by FTIR spectrometer (VERTEX 70, Bruker Spectrometer,

Germany) with the Potassium Bromide (KBr) tableting method (Ellerbrock and Gerke, 2004; Ellerbrock and Gerke, 2013). The sediment samples and KBr were dried at 100 °C for 6 h before tableting. Then 1 mg sediment sample together with 120 mg of KBr were ground in an agate mortar and mixed homogeneously. The infrared spectrum test ranged from 500 to 4000 cm^{-1} with resolution of 4 cm^{-1}, and each sample was scanned for 64 times. The atmosphere and CO_2 background are subtracted during the acquisition, and Omniic 8.0 was applied to perform baseline correction on the infrared spectrum. According to the infrared spectrum (i.e. each functional group has the specific absorption peaks), we divided the functional groups of SOM into five components including phenol & alcohol (3620, 3446 cm^{-1}), aliphatic carbon (2922, 2852, 1421 cm^{-1}), aromatic carbon (1639, 696 cm^{-1}), carbohydrates (1030 cm^{-1}) and organic silicon (798 cm^{-1}, Fig. S1) (Ellerbrock and Gerke, 2004; Ellerbrock and Gerke, 2013; Baumann et al., 2016), while obvious overlapping appeared in peaks affiliated with phenol & alcohol as well as carbohydrates. Thus, in order to semi-quantitatively analyse organic functional groups, we integrated the absorption peak and calculated its corrected area (Fig. S1). Finally, we calculated the percentage of each peak area (i.e. relative peak area of absorption).

2.6. DNA extraction and high throughput sequencing of the bacterial and archaeal communities

Total sediment DNA was extracted from approximately 0.5 g wet sediment sample (2–15 cm depth) using FastDNA SPIN Kit for soil (MP Biomedicals, USA) according to the manufacturer's protocol. The quality of extracted DNA was checked by 1% agarose gel electrophoresis. The universal primer set 515F (GTGCCAGCMGCCGCGGTAA) and 806R (GGACTACHVGGGTWTCTAAT) was employed to amplify the hypervariable V4 region of both bacterial and archaeal 16S rRNA genes (Angel et al., 2011; Kozich et al., 2013; Lever and Teske, 2015). PCR is divided into two rounds of amplification, and PCR products of appropriate size (~500 bp) were purified using Agencourt AMPure XP beads (Beckman, USA). The sequencing analysis entrusted Sangon Biotech (Shanghai, China) to perform high-throughput sequencing of the amplified gene fragments with the Illumina Miseq platform (Miseq 2×300 bp). Raw data were quality-filtered, chimera checked and clustered into operational taxonomic units (OTUs, 97% cutoff) using Usearch v9.2.64 (Edgar, 2010). Rarefaction curves and alpha diversity indices including Chao1, Shannon index and coverage were calculated in Mothur v1.30.1 (Schloss et al., 2009).

2.7. Metagenomic sequencing

Both the surface (0–2 cm) and the lower layer (5–10 cm) sediment samples of sampling site HS (HF reservoir) were applied for metagenomic sequencing. Metagenomic libraries were generated using the NEB Next Ultra DNA Library Prep Kit for Illumina (NEB, USA) following the manufacturer's protocols. The sequencing was performed on the Illumina Next Generation Sequencing Platform (paired-end 150 bp reads) at Sangon Biotech (Shanghai, China). A total of 27.6 Gb raw sequence data was generated (392,554,524 raw reads) from six metagenomes (three replicates for each depth). The raw metagenomic data was screened to remove adaptor fragments and low-quality reads and generate clean reads with Trimmomatic 0.36 (Bolger et al., 2014). Metagenomes were assembled using De Bruijn graph from IDBA-UD version 1.1.2 (Peng et al., 2012), and the trimmed reads were mapped to the contigs using Bowtie2 version 2.1.0 (Langmead and Salzberg, 2012). Contigs shorter than 1 kb or with an average coverage less than five were discarded from the assembly. The taxonomic assignment of the sequences was conducted using DIAMOND version 0.8.20 (Buchfink et al., 2015). The relative gene abundance was defined as the ratio of the sum of the sequencing depth of every base in the predicted gene to the gene length. Metabolism pathway analysis was performed using Kyoto Encyclopedia of Genes and Genomes (KEGG) (Kanehisa, 2004). We determined the relative abundance of methanogenesis-related functional genes based on the relative abundance of KEGG Orthology (KO) in KEGG database, and evaluated the relative ratios of different methanogenic pathways according to the modules of M00357, M00356, M00563 and M00567 in KEGG database (Z. Liu et al., 2018; Pyzik et al., 2018). Raw sequences of 16S rRNA genes and metagenomics reads have been made available in the NCBI Sequence Read Archive under the BioProject number PRJNA663741 and PRJNA663930, respectively.

2.8. Binning of metagenomic data

Metagenomic datasets generated for the two layers of sediment of HF reservoir were used in a combined assembly to recover genomes. High-quality metagenomic sequences were de novo assembled using SPAdes.v.3.12.0 (Nurk et al., 2017) with the following k-mer values: 21, 33, 55 and 77. The completeness, contamination, and strain heterogeneity of metagenome-assembled genomes (MAGs) were evaluated by using CheckM (version 1.0.5) (Parks et al., 2015). Species' annotation and classification of MAGs obtained by binning were based on GTDB-Tk database (Parks et al., 2018). For each predicted coding sequence, protein functions were annotated using the KEGG server (Kanehisa et al., 2016). Phylogenetic trees were constructed with recovered genome bins based on the results which used the FastTree algorithm with default settings by PhyloPhlAn (Price et al., 2009; Segata et al., 2013). The trees were visualized by using iTOL (Letunic and Bork, 2016), and rooted using the *Methanosarcina* as an out-group.

2.9. Statistical analysis

SPSS was used to perform all correlation coefficient analysis. The level of significance was $p < 0.05$ for all tests with SPSS. Origin 8.0 (OriginLab, USA) was used to plot the linear fit and relative abundance graphs. Principal Coordinate Analyses (PCoA) and Adonis analysis were performed to show the similarities and differences of microbial communities among different sediment samples. The canonical correspondence analysis (CCA) was used to analysis effects of biogeochemical parameters on the distribution of bacterial and archaeal communities. Mantel test was applied to evaluate the correlations of bacterial and archaeal communities with biogeochemical parameters. Network analysis was performed to investigate the co-occurrence patterns of bacterial and archaeal taxa (Barberan et al., 2012). All the analyses associated with microbial communities were performed using the R package Vegan (http://cran.r-project.org/web/packages/vegan/index.html).

3. Results

3.1. Sediment biogeochemical parameters and anaerobic decomposition of sediments organic matter in cascade reservoirs

The content of sediment organic carbon (SOC) in samples of HF reservoir ranged from 3.5% to 10.9%, most of them were significantly higher than that in WJD and DF reservoirs (2.9%–3.5%) (Table S3). The contents of total sulfur (TS) and nitrogen (TN) in most of the sediment samples of HF reservoir were also significantly higher compared with the other two reservoirs (Table S3). The C/N ratios of two sediment samples of HF reservoir were substantially higher than other samples (Table S3). The functional groups of SOC were mainly composed of carbohydrates, phenol & alcohol, aliphatic carbon, aromatic carbon and the lowest was organic silicon (Table S4). The SOC contents were positively correlated with the C/N ratios (Fig. S2a), as well as the contents of aromatic and aliphatic carbon of SOM (Fig. 3d and e). However, the SOC contents were negatively correlated with the contents of carbohydrates (Fig. 3f).

When normalized to sediment volume, the methane production rates (MPR) in sediment samples of HF reservoir (at 15 °C) ranged from 0.15 to 0.54 μmol cm^{-3} d^{-1} (Fig. 2a), while that in WJD and DF reservoirs ranged from 0.11 to 0.34 μmol cm^{-3} d^{-1} (Fig. 2a). The MPR at 25 °C

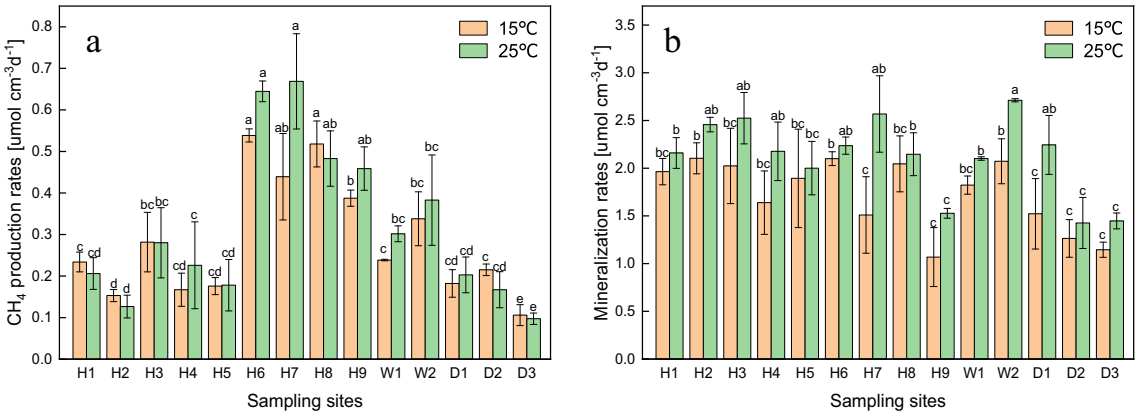

Fig. 2. Average methane production rates (a) and mineralization rates (b) of sediment samples incubated under 15 °C and 25 °C in three cascade reservoirs, normalized to sediment volume. Error bar denotes the standard deviation (SD) of the mean (n = 3). Different letters on the top of the column indicates significant difference among the sampling sites (Tukey's HSD; $P < 0.05$). H, W and D denote sampling sites of Hongfeng, Wujiangdu and Dongfeng reservoirs, respectively.

(0.10–0.67 μmol cm^{-3} d^{-1}) were slightly higher than at 15 °C. The mineralization rate of sediment samples were similar among different reservoirs, but fluctuated from 1.07 to 2.10 μmol cm^{-3} d^{-1} (at 15 °C) among different sampling sites (Fig. 2b), and the mineralization rates were generally higher at elevated temperature (1.43–2.71 μmol cm^{-3} d^{-1}, Fig. 2b). The SOC contents were positively correlated with MPR, but had no correlation with total CO_2 production or mineralization rates of sediment at 15 °C, while the SOC contents had slight positive correlation with mineralization rates of sediment at 25 °C (Fig. 3a–c). Meantime, C/N, TN and TS were also positively correlated with MPR (Fig. S2).

In contrast, when normalized to SOC, the MPR at 15 °C (ranged from 5.9 to 24.0 μmol g SOC^{-1} d^{-1}) were similar among the three reservoirs (Fig. S3a), while the total CO_2 production rates (ranged from 9.4 to 197.4 μmol g SOC^{-1} d^{-1}) were substantially lower in four sampling sites (H6-H9) of HF (Fig. S3b). The MPR normalized by SOC were not significantly correlated with the SOC contents, and also hardly correlated with C/N ratios of the sediment (Fig. S3c and e). While the total CO_2 production rates normalized by SOC were negatively correlated with SOC contents and C/N ratios (Fig. S3d and f).

3.2. Compositions of bacterial and archaeal communities in sediments of cascade reservoirs

The compositions of bacterial and archaeal communities in reservoir sediments were analyzed by high throughput sequencing of 16S rRNA genes. After quality control, 91,737 to 242,153 high quality sequences were yielded for each sediment sample (Table S5). And the alpha diversity indexes of 16S rRNA genes were significantly correlated with the biogeochemical parameters, including TN, SOC, TS, Fe (II), hydraulic residence time (HRT) (Table S6). Phylogenetic analysis indicated that the

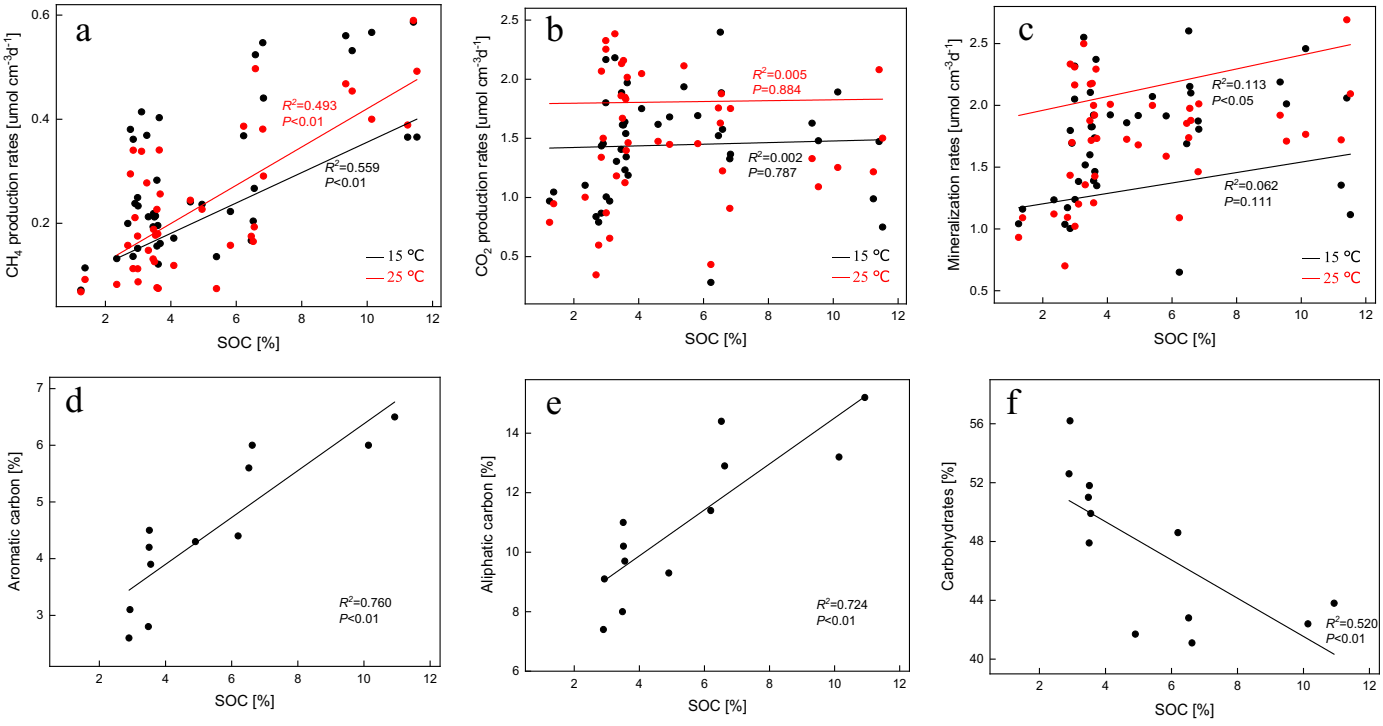

Fig. 3. Pearson's correlation coefficients between sediment organic carbon (SOC) contents and biogeochemical parameters, including methane production rates (a), total CO_2 production rates (b), mineralization rates of sediment samples when normalized to sediment volume (c), as well as the relative contents of aromatic carbon (d), aliphatic carbon (e) and carbohydrates (f) of SOM. The sediment samples were incubated under 15 °C and 25 °C, all the data from every reservoir was included for the analyses.

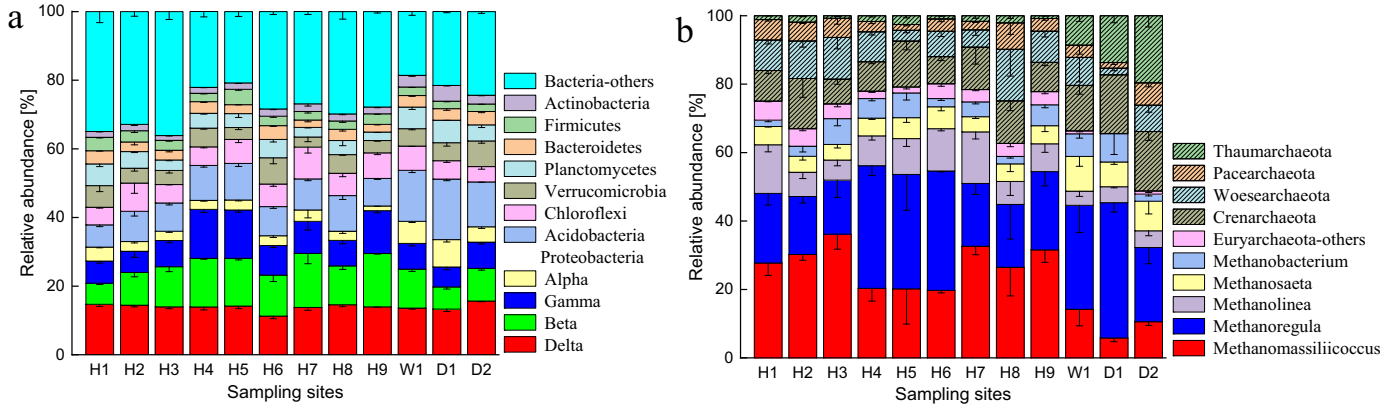

Fig. 4. Average relative sequence abundances of bacterial phyla and classes (a), as well as archaeal phyla and main methanogens genera (b). Column "Bacteria-others" indicates combined relative sequence abundances of all the rare phyla, candidate divisions and of the taxonomically unclassified sequences; rare phyla were defined as having average relative sequence abundances between all samples of <1%. Column "*Euryarchaeota-others*" indicates non-methanogens in *Euryarchaeota*. Error bars indicate the SD of means (n = 3). H, W and D denote sampling sites of Hongfenghu, Wujiangdu and Dongfeng reservoirs, respectively.

relative abundances of bacteria and archaea were about 93.3%–98.6% and 1.7%–6.7% in these sediment samples (Table S7), respectively.

For bacterial communities, *Proteobacteria* was the most predominant phylum in all sites with a proportion ranging from about 30% to 50% (Fig. 4a). For archaea, the dominant phylum was *Euryarchaeota* with a proportion ranging from about 40% to 85% (Fig. 4b), it mainly consisted of several genera of methanogens, such as *Methanomassiliicoccus*, *Methanoregula*, *Methanolinea*, and *Methanosaeta*. Besides, the results also showed that the reservoir sediment samples contained other four archaeal phyla, including *Crenarchaeota*, *Woesearchaeota*, *Pacearchaeota* and *Thaumarchaeota*.

3.3. Biogeochemical parameters shaping the microbial community structures

Principal coordinate analysis (PCoA) (explained 45% variances) showed that the compositions of bacterial communities of the sediment

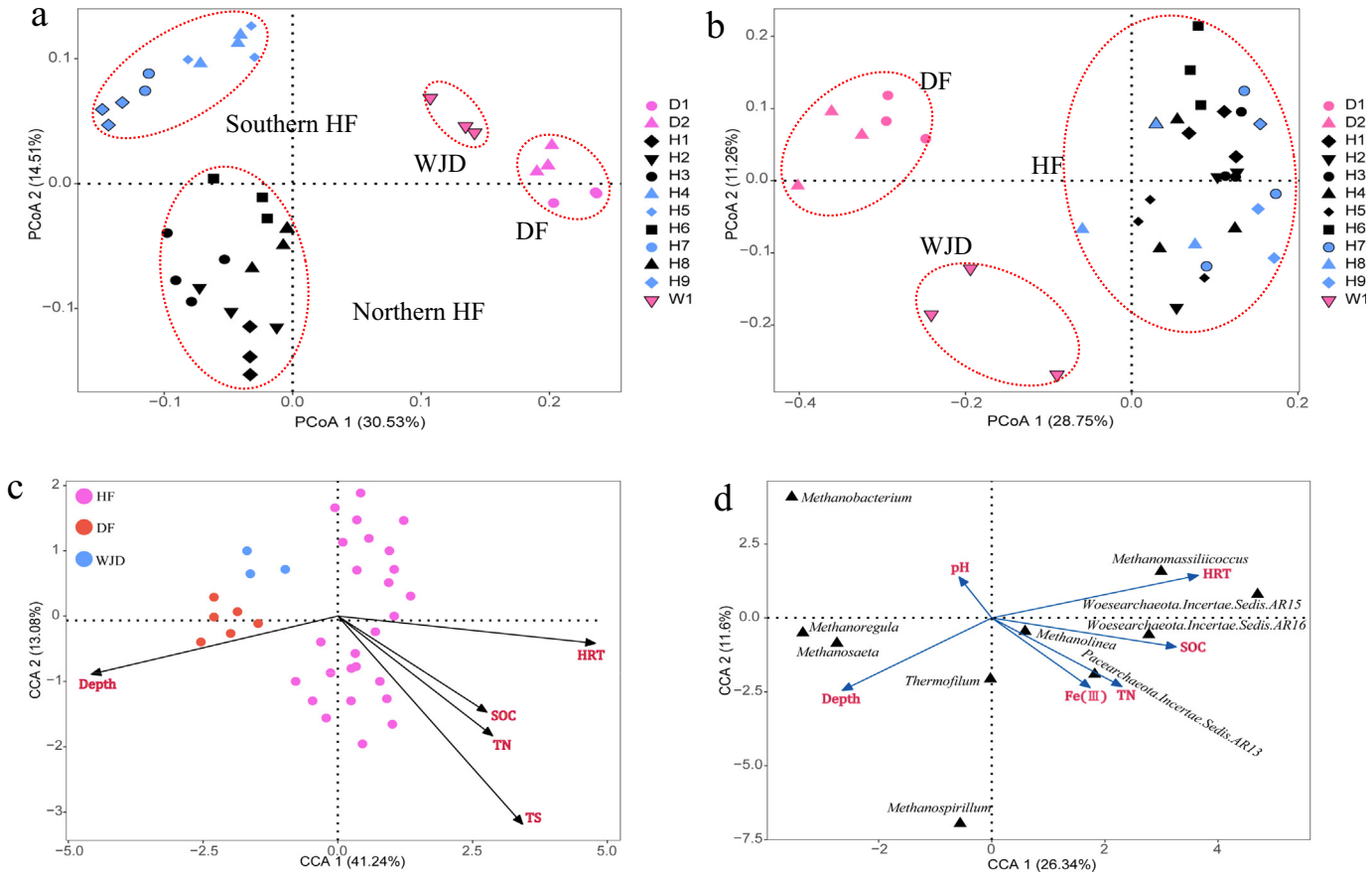

Fig. 5. Principal coordinate analysis (PCoA) of bacterial (a) and archaeal (b) communities based on the unweighted UniFrac distance metric. And Canonical correspondence analysis (CCA) of the effects of biogeochemical parameters on bacterial (c) and archaeal (d) communities. The dominant bacterial and archaeal genera (average relative sequence abundances >0.1%) were used as input. Northern HF, southern HF, DF and WJD denote sampling sites of northern area of Hongfeng, the southern area of Hongfeng, Dongfeng and Wujiangdu reservoirs, respectively. Arrows indicate the direction and magnitude of biogeochemical variables associated with dominant community structures. Abbreviations: HRT, hydraulic residence time; TN, total nitrogen; TS, total sulfur; SOC, sediment organic carbon.

samples were separated into four groups of DF, WJD, Northern HF and Southern HF (Fig. 5a and Table S8). Similarly, composition of archaeal communities were separated based on the reservoirs (Fig. 5b and Table S8). Meantime, based on the canonical correspondence analysis (CCA) (explained 54% variances), depth significantly affected the bacterial community structures of DF and WJD reservoirs (Fig. 5c). HRT together with SOC, TN and TS significantly affected the bacterial community structures of HF reservoir (Fig. 5c). The partial mantel test also showed that HRT had highest correlations with prokaryotic community structures of these sediment samples (Table S9). Furthermore, CCA analysis of archaeal communities (explained 38% variances) indicated that the *Methanoregula* and *Methanosaeta* were largely affected by water depth, while *Methanomassiliicoccus* and *Woesearchaeota* were mainly controlled by HRT (Fig. 5d).

3.4. Microbial co-occurrence network analysis

In order to characterize the correlation of bacterial and archaeal microorganisms in these sediment samples, a positive correlation-based network was constructed with the most abundant 100 prokaryotic genera (Fig. 6). About half of the nodes were grouped into *Proteobacteria* (35%) and methanogens (8%) (Fig. 6 and Table S10). The prokaryotic community in the network was organized by three major functional modules (Fig. 6). Among them, module I was composed of both

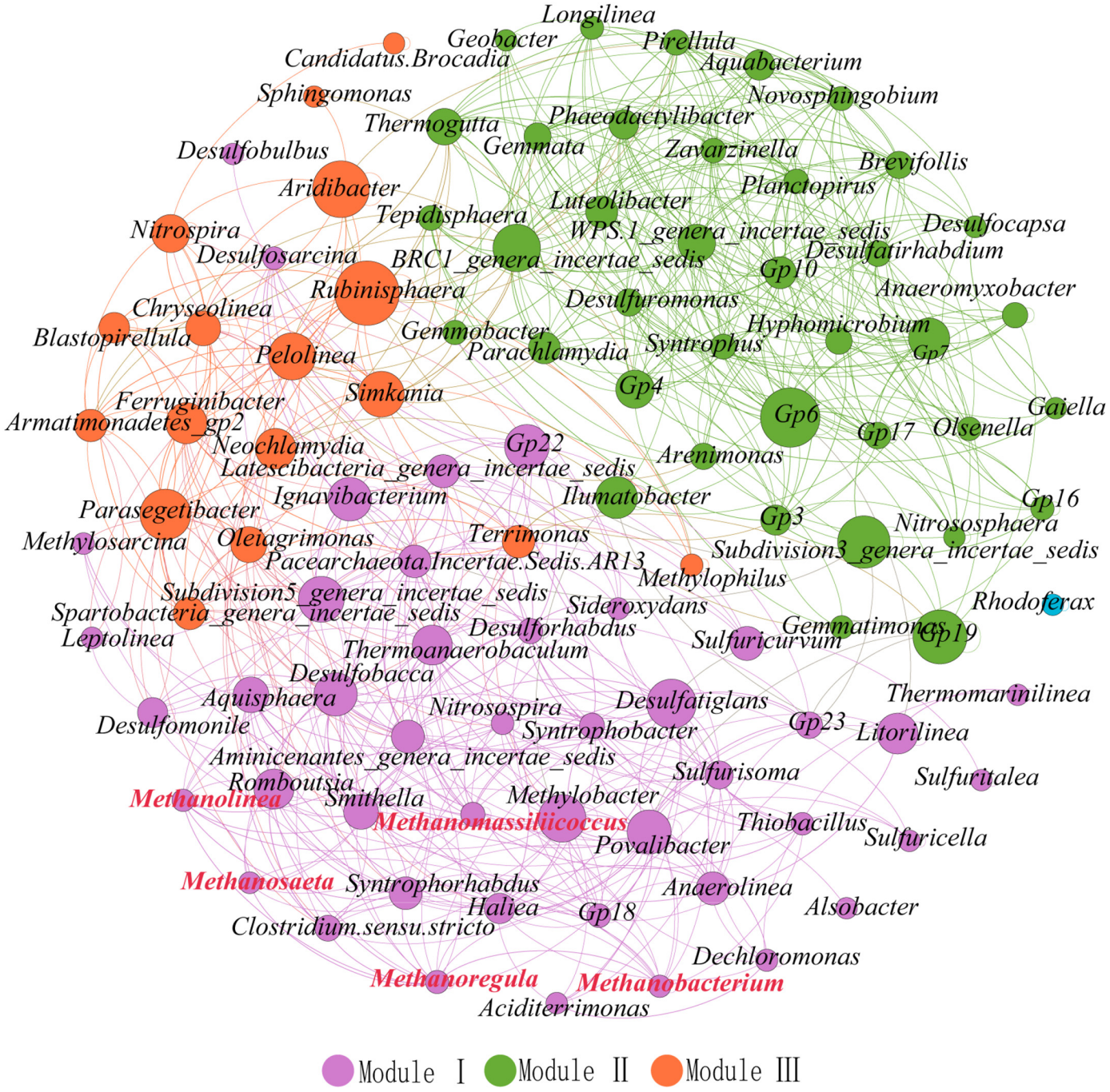

Fig. 6. Network of co-occurring bacterial and archaeal genera based on Spearman correlation analysis sorted in color by modularity class. A connection stands for a significant ($R > 0.6$, $P < 0.01$) correlation. The size of each node (genus) is proportional to its relative abundance, the thickness of each connection between two nodes (edge) is proportional to the corresponding correlation coefficient. Methanogens are marked in bold and red.

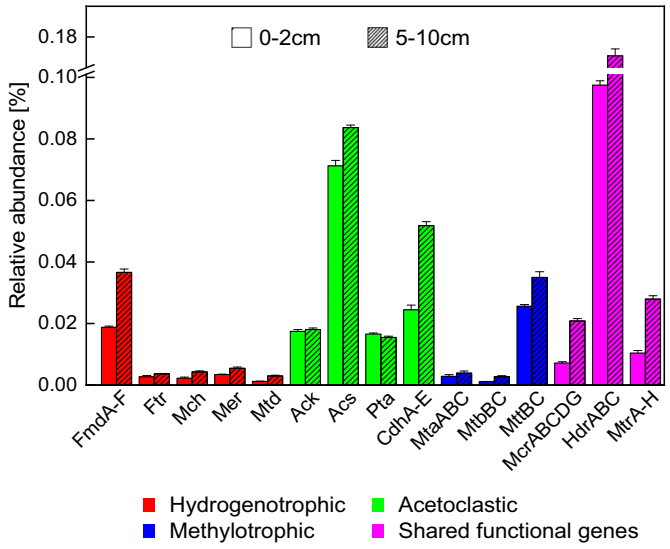

Fig. 7. Relative abundance of methanogenesis-related genes in surface (0–2 cm) and lower layer (5–10 cm) of the reservoir sediment samples. The three methanogenic pathways are represented by different colors. The shared functional genes denote genes common for all pathways. FmdA-F (formylmethanofuran dehydrogenase (subunits ABCDEF)), Ftr (formylmethanofuran-H4MPT formyltransferase), Mer (5,10-methylene-H4MPT reductase), Mtd (methylene-5,6,7,8-H4MPT dehydrogenase). Ack (acetate kinase), Acs (acetyl-CoA synthetase), Pta (phosphate acetyltransferase), CdhA-E (CO dehydrogenase/acetyl-CoA synthase (subunits ABCDE)). MtaABC (methanol-specifc methyltransferase complex (subunits ABC)), MtbBC (dimethylamine-corrinoid protein Co-methyltransferase (subunits BC)), MttBC (trimethylamine-corrinoid protein Co-methyltransferase (subunits BC)). McrABCDG (methyl CoM reductase (subunits ABCDG)), HdrABC (CoB-CoM heterodisulfde reductase (subunits ABC)), MtrA-H (H4MPT-methyltransferase (subunits ABCDEFH)). The relative abundances (%) were calculated from KEGG database using data of metagenomic sequencing. Error bar denotes the SD of the mean (n = 3).

bacterial and methanogenic archaea, while module II and III were exclusively composed of bacterial nodes (Table S10).

3.5. Metagenomic analysis of methanogenic archaea in the sediment samples

In order to get a deeper understanding of methanogenic archaea in the reservoir sediments, metagenomic analysis was performed for the sediment samples of HF reservoir, which had more active methane production and higher relative abundance of methanogenic archaea compared with the other two reservoirs (Figs. 2a and 4b). The results showed that compared with the surface sediment, the relative abundances of genes associated with each methanogenesis pathway were generally higher in lower layer sediment (Fig. 7). The relative abundances of genes of FmdA-F (hydrogenotrophic pathway), MttBC (methylotrophic pathway), Acs and CdhA-E (acetoclastic pathway) were apparently higher compared with other genes which affiliated with the three methanogenesis pathways. Meanwhile, the total relative abundances of genes involved in methylotrophic methanogenic pathways were similar with that in acetoclastic pathways in both surface and lower layer sediment, while the relative abundances of hydrogenotrophic pathway were slightly lower (Fig. S5).

De novo genomic assembly and binning of metagenome sequencing data resulted in the reconstruction of 4 metagenome-assembled genomes (MAGs) affiliated with *Euryarchaeota* methanogens in the sediments of HF reservoir (Table 1). To identify lineages of these MAGs, we constructed phylogenetic trees based on a concatenated set of 16S ribosomal protein sequences (Fig. S6). All the MAGs clustered within the genus *Methanoregula*. Meanwhile, MAGs annotation revealed that they possessed genes encoding conserved core enzymes of hydrogenotrophic methanogenesis, including Fwd, Ftr, Mch, Mtd, Mer, Mtr, and Mcr (Additional file 1). They also had a large number of electron transporters encoded in their genomes. In addition, they encoded multiple membrane-bound hydrogenases as well as lipooligosaccharide and monosaccharide transporters (Additional file 1).

4. Discussion

4.1. Methanogenesis activity in the sediment of cascade reservoirs

Cascade damming on a river will produce a series of reservoirs substantially different in biogeochemical characteristics. Especially, the much longer hydraulic residence time (HRT) in HF reservoir (119 days) will lead to higher sedimentation rates of both terrestrial and aquatic particulate substances (Groeger and Kimmel, 1984; Maavara et al., 2015; Y. Zhao et al., 2020; Z. Zhao et al., 2020). As a result, the sediment of the HF reservoir is rich in sediment organic carbon (SOC) as well as total sulfur (TS) and nitrogen (TN) (Table S3). The relatively large fluctuations in contents of SOC (3.5%–10.9%), TS (0.2%–1.2%) and TN (0.3%–8%) (Table S3) in HF reservoir could be attributed to its substantially larger surface area (Table S1) (Y. Zhao et al., 2020), as well as its longer HRT which could accelerate the sedimentation of particles and reduce their migration within the reservoir. Then, sediments of HF reservoir could supply richer and spatially heterogeneous substrates for methane production after anaerobic mineralization.

As a result, sediment samples of HF reservoir had higher relative abundance of methanogens, greater diversity of bacterial and archaeal communities (Figs. 4 and 5), and several samples largely enriched in SOC exhibited significantly stronger methane production rates (MPR) when normalized to sediment volume (Fig. 2a and Table S3). This could explain the positive correlation of biogeochemical parameters (including SOC, TS and TN) with MPR normalized by sediment volume (Fig. 3a and Fig. S2), as well as with the bacterial and archaeal communities (Fig. 5 and Table S6). Nevertheless, more sampling sites from DF and WJD reservoirs would be helpful for consolidating the importance of HRT. The MPR of these cascade reservoirs (0.07 to 0.87 μmol cm^{-3} d^{-1}) (Fig. 2a) were similar or slightly lower than those reported in other lakes and reservoirs. For example, the MPR of the sediment of William H. Harsha Lake were 0.62–1.23 μmol cm^{-3} d^{-1} (Berberich et al., 2020), and that of the four cascade hydropower reservoirs located at the upstream of Mekong River were 0.09–0.88 μmol $cm^{-3}d^{-1}$ (Liu et al., 2020).

Generally, C/N ratio could be used to identify sources of organic matter in sediment (Meyers and Ishiwatari, 1993; Meyers, 1994; Chen et al., 2002), since the C/N ratios of aquatic algae are usually less than 10,

Table 1
Characteristics of four MAGs of methanogens reconstructed in this study.

Bin ID	Size (Mbp)	Compl. (%)	Cont. (%)	Strain hetero.	Scaffolds (no.)	Genes (no.)	GC (%)	Longest scaffold (kbp)
H13bin3	0.58	45.72	1.31	100	143	698	49.10	106.84
H21bin13	1.20	72.56	0.16	100	242	1402	48.67	175.44
H22bin6	0.98	58.52	0.65	100	221	1139	48.65	119.35
H23bin3	1.03	72.39	1.57	50	222	1223	48.91	192.78

The following are shown: *Compl.* estimated completeness, *Cont.* estimated contamination, *Strain hetero.* strain heterogeneity, number of scaffolds, number of protein-coding genes, and *GC* guanine-cytosine content.

while that of terrestrial plants are greater than 15 (Meyers and Ishiwatari, 1993; Chen et al., 2002; Cloern et al., 2002). Therefore, the substantial variations of C/N ratios (8.1–25.5) (Table S3) as well as the significant positive correlation between SOC contents and C/N ratios (Fig. S2) suggested that terrestrial input greatly enhanced the accumulation of SOC (Meyers, 1994; Cloern et al., 2002), and resultantly stimulated the CH_4 production of the sediment. Nevertheless, terrestrial organic matters were considered more difficult to be decomposed than aquatic organic matters (Blair and Aller, 2012; Grasset et al., 2018; Wei et al., 2020) mainly because of their higher contents of lignin, which was very difficult to break down under anaerobic condition (Dai, 2005; Jia et al., 2013; Grasset et al., 2018). Indeed, the contents of recalcitrant components, e.g. aromatic and aliphatic carbon (Ellerbrock and Gerke, 2013; Jiang et al., 2018), in the sediment organic matter were positively correlated with SOC contents of the sediment samples (Fig. 3d and e). Resultantly, when normalized to sediment volume, the MPR but not the SOC mineralization rates significantly increased together with the SOC contents (Fig. 3a and c). This could be explained by that the SOC with higher recalcitrant carbon undergo incomplete mineralization under anaerobic conditions, which may preferentially produce CH_4 rather than CO_2 (Conrad et al., 2009). This was in agreement with that the CO_2 production rates normalized by SOC were negatively correlated with both the SOC contents and C/N ratios ($P < 0.01$) (Fig. S3d and f). These results suggested that cascade reservoirs are favorable for the burial of terrestrial organic carbon even though higher SOC stimulated MPR of the sediments. Recent study in coastal oceans also showed that terrigenous organic carbon is more persistent and its preservation in the marine system is better than previously thought (Blair and Aller, 2012; Tesi et al., 2016; Hemingway et al., 2019; Wei et al., 2020).

4.2. Compositions of methanogenic archaeal populations in the sediment of cascade reservoirs

For these cascade reservoirs, oxygen could penetrate into the surface sediments (normally a few millimeters) because there is usually relatively high dissolved oxygen content in the water column (Bryant et al., 2010; X.L. Liu et al., 2018; Wang et al., 2018b). Our results also indicated that there were lower abundances of functional genes involved in methanogenesis in the surface sediment of 0–2 cm depth (Fig. 7). Meanwhile, previous studies showed that the seasonal dynamics of abundance and structure of methanogenic communities were detected at the superficial sediment (within 0–2 cm depth) but not at the sediment of lower depth (Chan et al., 2005; Lyautey et al., 2021). On the other hand, our pre-experiments with sediment of different depth showed that the methane production potential of the sediment apparently decreased below 20 cm depth (Fig. S4). So, this study targeted on the sediment of 2–15 cm depth, since it should represent the highest methane production potential of the sediment samples. Besides, our results should be able to reflect the typical methanogenic communities of the 2–15 cm depth even though we only sampled at one time point.

In sediments of freshwater ecosystems, the dominant methanogens usually belong to acetoclastic and hydrogenotrophic methanogenesis, including *Methanoregula* and *Methanosaeta* (Biderre-Petit et al., 2011; Borrel et al., 2011; Youngblut et al., 2014). Our results also indicated that the hydrogenotrophic methangen *Methanoregula* was abundant in the sediment of cascade reservoirs (Fig. 4b). Moreover, the MAGs analysis showed that the genomes of *Methanoregula* encoded large number of electron transporters (Additional file 1), this was consistent with results of comparative genomic analysis which suggested the metabolic adaptation of *Methanoregula* to low substrate (H_2) concentrations (Browne et al., 2017). In addition, *Methanoregula* encoded multiple lipooligosaccharide and monosaccharide transporters (Additional file 1), which illustrated that the *Methanoregula* in sediment of cascade reservoirs might adaptation to a heterotrophic lifestyle (Zhang et al., 2020). Meanwhile, the *Methanosaeta* was almost the sole acetoclastic methanogen presented in the reservoir sediment (Fig. 4b).

Last but not least, the dominant methanogen groups in our study included methylotrophic *Methanomassiliicoccus* (Fig. 4b) (Evans et al., 2019) which can grow with methylamines (methylamine, dimethylamine, trimethylamine) in the presence of H_2 (Borrel et al., 2014a). *Methanomassiliicoccus* is a subgroup of *Thermoplasmata* and is phylogenetically distant from other methanogens (Borrel et al., 2014b). Moreover, metagenomic analysis of both surface and lower layer sediment samples also showed the relative abundance of functional genes affiliated with methylotrophic methanogenesis were comparable with hydrogenotrophic and acetoclastic methanogenesis (Fig. 7 and Fig. S5), further suggested that methylotrophic methanogenesis might play an important role in methane production of the sediment of cascade reservoirs. In fact, the order *Methanomassiliicoccales* are usually relatively abundant in saline environments (e.g. mangrove ecosystems) with relative abundance of up to about 40% of total methanogenic community (Pan et al., 2019; Zhang et al., 2020), but it's usually less than 6% in freshwater lakes (Chan et al., 2005; Fan et al., 2018; Kadnikov et al., 2019). In contrast, our study showed that the *Methanomassiliicoccus* had a relatively higher proportion, which was about 8–49% of total methanogenic community, in the sediment of cascade reservoirs. Therefore, our results suggested that cascade reservoirs might be one of the few freshwater ecosystems suitable for the flourishing of methylotrophic methanogens. The plausible reason could be that cascade damming is also favorable for the accumulation of inorganic elements (Campo and Sancholuz, 1998; Humborg et al., 2002), which might increase the salinity of reservoir water. Previous studies did show that the interception effect of the cascade reservoirs in the Wujiang River basin was conducive to the accumulation of F^-, SO_4^{2-}, Cl^-, Ca^{2+} and Mg^{2+} (Han and Liu, 2004; Li and Ji, 2016; Huang et al., 2017; Z. Zhao et al., 2020). Nevertheless, relative abundance of methanogens doesn't necessarily reflect their metabolic activity, further investigations based on carbon isotopes and substrate addition (Conrad et al., 2009; Zhuang et al., 2018) are helpful for confirming the role of methylotrophic methanogens in these reservoirs.

4.3. Microbial co-occurrence patterns

In general, positive co-occurrence of prokaryotic populations within or between modules could reflect their similar niche adaptation or interspecies cooperation (Rui et al., 2015). For this study, methanogens were presented only in module I together with bacteria mainly composed of fermentative and syntrophic bacteria, as well as sulfate reducing bacteria (SRB) (Fig. 6). The numerous positive correlations between methanogens and bacteria in module I were probably caused by the production of methanogenic substrates (H_2/CO_2, formate and acetate) from the fermentative bacteria, such as *Smithella* and *Anaerolinea* (Yamada et al., 2007; Liang et al., 2015; Rui et al., 2015; Yongkyu et al., 2015; Wawrik et al., 2016), or because of multiple interactions between syntrophic bacteria (e.g. *Syntrophobacter* and *Syntrophorhabdus*) and hydrogenotrophic methanogens (Schink, 1997; Gray et al., 2011; Worm et al., 2014; Nobu et al., 2015; Sedano-Nunez et al., 2018). As for SRB, including *Thiobacillus* and *Desulforhabdus* here in module I, they compete electron donors (H_2 and acetate) but share similar niches with methanogens in rich organic matter environments (Oremland et al., 1982; Robinson and Tiedje, 1984). Besides, the positive correlation between *Methanomassiliicoccus* and SRB could be explained by that methylotrophic methanogens might coexist with sulfate reducers, because acetate and hydrogen are often utilized by sulfate-reducing bacteria, while methyl compounds are exclusively utilized by methylotrophic methanogens (Zhuang et al., 2018).

5. Conclusions

Our results suggested that methylotrophic methanogenesis might play an important role in methane production in the sediment of cascade reservoirs. In addition, the hydraulic residence time could be the

key controlling factor of structures of bacterial and archaeal communities as well as CH_4 production rates of the reservoir sediments. At last, terrestrial organic matter largely stimulates the CH_4 production from the reservoir sediments although it's recalcitrant to decomposition. Further studies on more cascade reservoirs will be helpful for a deeper interpretation of the anaerobic decomposition of organic matter as well as methanogenic community in the reservoir sediments.

The following are the supplementary data related to this article.

CRediT authorship contribution statement

Debin Wu: Resources, Investigation, Formal analysis, Writing – original draft, Writing – review & editing. **Yuan Zhao:** Resources, Investigation. **Lei Cheng:** Resources, Formal analysis. **Zhuo Zhou:** Resources, Formal analysis. **Qiusheng Wu:** Formal analysis, Visualization. **Qian Wang:** Resources, Investigation. **Quan Yuan:** Funding acquisition, Conceptualization, Writing – original draft, Writing – review & editing.

Declaration of competing interest

The authors declare that they have no known competing financial interests or personal relationships that could have appeared to influence the work reported in this paper.

Acknowledgements

This work was supported by the National Key Research and Development Program of China [No. 2016YFA0601000]; by the National Natural Science Foundation of China [No. 41573083 and U1612441].

Appendix A. Supplementary data

Supplementary data to this article can be found online at https://doi.org/10.1016/j.scitotenv.2021.147515.

References

Angel, R., Claus, P., Conrad, R., 2011. Methanogenic archaea are globally ubiquitous in aerated soils and become active under wet anoxic conditions. ISME J. 6, 847–862.

Barberan, A., Bates, S.T., Casamayor, E.O., Fierer, N., 2012. Using network analysis to explore co-occurrence patterns in soil microbial communities. ISME J. 6, 343–351.

Barros, N., Cole, J.J., Tranvik, L.J., Prairie, Y.T., Bastviken, D., Huszar, V.L.M., del Giorgio, P., Roland, F., 2011. Carbon emission from hydroelectric reservoirs linked to reservoir age and latitude. Nat. Geosci. 4, 593–596.

Bastviken, D., Cole, J.J., Pace, M.L., Van de Bogert, M.C., 2008. Fates of methane from different lake habitats: connecting whole-lake budgets and CH_4 emissions. Biogeosciences. 113, 1–13.

Baumann, K., Schöning, I., Schrumpf, M., Ellerbrock, R.H., Leinweber, P., 2016. Rapid assessment of soil organic matter: soil color analysis and Fourier transform infrared spectroscopy. Geoderma. 278, 49–57.

Berberich, M.E., Beaulieu, J.J., Hamilton, T.L., Waldo, S., Buffam, I., 2020. Spatial variability of sediment methane production and methanogen communities within a eutrophic reservoir: importance of organic matter source and quantity. Limnol. Oceanogr. 65, 1–23.

Biderre-Petit, C., Jézéquel, D., Dugat-Bony, E., Lopes, F., Kuever, J., Borrel, G., Viollier, E., Fonty, G., Peyret, P., 2011. Identification of microbial communities involved in the methane cycle of a freshwater meromictic lake. FEMS Microbiol. Ecol. 77, 533–545.

Blair, N.E., Aller, R.C., 2012. The fate of terrestrial organic carbon in the marine environment. Annu. Rev. Mar. Sci. 4, 401–423.

Bolger, A.M., Lohse, M., Usadel, B., 2014. Trimmomatic: a flexible trimmer for Illumina sequence data. Bioinformatics 30, 2114–2120.

Borrel, G., Jézéquel, D., Biderre-Petit, C., Morel-Desrosiers, N., Morel, J.-P., Peyret, P., Fonty, G., Lehours, A.-C., 2011. Production and consumption of methane in freshwater lake ecosystems. Res. Microbiol. 162, 832–847.

Borrel, G., Gaci, N., Peyret, P., O'Toole, P.W., Gribaldo, S., Brugère, J.-F., 2014a. Unique characteristics of the pyrrolysine system in the 7th order of methanogens: implications for the evolution of a genetic code expansion cassette. Archaea 2014, 1–11.

Borrel, G., Parisot, N., Harris, H.M.B., Peyretaillade, E., Gaci, N., Tottey, W., Bardot, O., Raymann, K., Gribaldo, S., Peyret, P., O'Toole, P.W., Brugère, J.-F., 2014b. Comparative genomics highlights the unique biology of Methanomassiliicoccales, a Thermoplasmatales-related seventh order of methanogenic archaea that encodes pyrrolysine. BMC Genomics 15, 679.

Browne, P., Tamaki, H., Kyrpides, N., Woyke, T., Goodwin, L., Imachi, H., Brauer, S., Yavitt, J.B., Liu, W.T., Zinder, S., Cadillo-Quiroz, H., 2017. Genomic composition and dynamics among Methanomicrobiales predict adaptation to contrasting environments. ISME J. 11, 87–99.

Bryant, L.D., Lorrai, C., McGinnis, Daniel F., Brand, A., est, A.W., Little, J.C., 2010. Variable sediment oxygen uptake in response to dynamic forcing. Limnol. Oceanogr. 55, 950–964.

Buchfink, B., Xie, C., Huson, D.H., 2015. Fast and sensitive protein alignment using DIAMOND. Nat. Methods 12, 59–60.

Campo, J., Sancholuz, L., 1998. Biogeochemical impacts of submerging forests through large dams in the Río Negro, Uruguay. J. Environ. Manag. 54, 59–66.

Chan, O.C., Claus, P., Casper, P., Ulrich, A., Lueders, T., Conrad, R., 2005. Vertical distribution of structure and function of the methanogenic archaeal community in Lake Dagow sediment. Environ. Microbiol. 7, 1139–1149.

Chen, J., Wan, G., Wang, F., Zhang, D.D., Huang, R., Zhang, F., Schmidt, R., 2002. Environmental records of carbon in recent lake sediments. Sci. China 45, 875–884.

Chen, Q., Chen, J., Wang, J., Guo, J., Jin, Z., Yu, P., Ma, Z., 2019. In situ, high-resolution evidence of phosphorus release from sediments controlled by the reductive dissolution of iron-bound phosphorus in a deep reservoir, southwestern China. Sci. Total Environ. 666, 39–45.

Cloern, J.E., Canuel, E.A., Harris, D., 2002. Stable carbon and nitrogen isotope composition of aquatic and terrestrial plants of the San Francisco Bay estuarine system. Limnol. Oceamogr. 47, 713–729.

Conrad, R., 1999. Contribution of hydrogen to methane production and control of hydrogen concentrations in methanogenic soils and sediments. FEMS Microbiol. Ecol. 28, 193–202.

Conrad, R., 2009. The global methane cycle: recent advances in understanding the microbial processes involved. Environ. Microbiol. Rep. 1, 285–292.

Conrad, R., 2020. Importance of hydrogenotrophic, aceticlastic and methylotrophic methanogenesis for methane production in terrestrial, aquatic and other anoxic environments: a mini review. Pedosphere 30, 25–39.

Conrad, R., Chan, O.-C., Claus, P., Casper, P., 2007. Characterization of methanogenic Archaea and stable isotope fractionation during methane production in the profundal sediment of an oligotrophic lake (Lake Stechlin, Germany). Limnol. Oceanogr. 52, 1393–1406.

Conrad, R., Claus, P., Casper, P., 2009. Characterization of stable isotope fractionation during methane production in the sediment of a eutrophic lake, Lake Dagow, Germany. Limnol. Oceanogr. 54, 457–471.

Dai, J., 2005. Changes in chemical and isotopic signatures of plant materials during degradation: implication for assessing various organic inputs in estuarine systems. Geophys. Res. Lett. 32, 1–4.

Dean, W.E., Gorham, E., 1998. Magnitude and significance of carbon burial in lakes, reservoirs, and peatlands. Geology. 26, 535.

Deemer, B.R., Harrison, J.A., Li, S., Beaulieu, J.J., DelSontro, T., Barros, N., Bezerra-Neto, J.F., Powers, S.M., dos Santos, M.A., Vonk, J.A., 2016. Greenhouse gas emissions from reservoir water surfaces: a new global synthesis. BioScience 66, 949–964.

Edgar, R.C., 2010. Search and clustering orders of magnitude faster than BLAST. Bioinformatics. 26, 2460–2461.

Ellerbrock, R.H., Gerke, H.H., 2004. Characterizing organic matter of soil aggregate coatings and biopores by Fourier transform infrared spectroscopy. Eur. J. Soil Sci. 55, 219–228.

Ellerbrock, R.H., Gerke, H.H., 2013. Characterization of organic matter composition of soil and flow path surfaces based on physicochemical principles—a review. Adv. Agron. 121, 117–177.

Evans, P.N., Boyd, J.A., Leu, A.O., Woodcroft, B.J., Parks, D.H., Hugenholtz, P., Tyson, G.W., 2019. An evolving view of methane metabolism in the Archaea. Nat. Rev. Microbiol. 17, 219–232.

Falz, K.Z., Holliger, C., Grosskopf, R., Liesack, W., Hahn, D., 1999. Vertical distribution of methanogens in the anoxic sediment of Rotsee (Switzerland). Appl. Environ. Microbiol. 65, 2402–2408.

Fan, L., Wu, W., Qiu, L., Song, C., Meng, S., Zheng, Y., Hu, G., Li, D., Chen, J., 2018. Methanogenic community compositions in surface sediment of freshwater aquaculture ponds and the influencing factors. Antonie Van Leeuwenhoek 111, 115–124.

Grasset, C., Mendonça, R., Villamor Saucedo, G., Bastviken, D., Roland, F., Sobek, S., 2018. Large but variable methane production in anoxic freshwater sediment upon addition of allochthonous and autochthonous organic matter. Limnol. Oceanogr. 63, 1488–1501.

Gray, N.D., Sherry, A., Grant, R.J., Rowan, A.K., Hubert, C.R., Callbeck, C.M., Aitken, C.M., Jones, D.M., Adams, J.J., Larter, S.R., Head, I.M., 2011. The quantitative significance of Syntrophaceae and syntrophic partnerships in methanogenic degradation of crude oil alkanes. Environ. Microbiol. 13, 2957–2975.

Groeger, A.W., Kimmel, B.L., 1984. Organic matter supply and processing in lakes and reservoirs. Lake Res. Manag. 1, 282–285.

Gruca-Rokosz, R., Tomaszek, J.A., 2015. Methane and carbon dioxide in the sediment of a eutrophic reservoir: production pathways and diffusion fluxes at the sediment-water interface. Water Air Soil Pollut. 226, 16.

Han, G., Liu, C.-Q., 2004. Water geochemistry controlled by carbonate dissolution: a study of the river waters draining karst-dominated terrain, Guizhou Province, China. Chem. Geol. 204, 1–21.

Hayes, N.M., Deemer, B.R., Corman, J.R., Razavi, N.R., Strock, K.E., 2017. Key differences between lakes and reservoirs modify climate signals: a case for a new conceptual model. Limnol. Oceanogr. Lett. 2, 47–62.

Hemingway, J.D., Rothman, D.H., Grant, K.E., Rosengard, S.Z., Eglinton, T.I., Derry, L.A., Galy, V.V., 2019. Mineral protection regulates long-term global preservation of natural organic carbon. Nature 570, 228–231.

Huang, Q.B., Qin, X.Q., Liu, P.Y., Zhang, L.K., Su, C.T., 2017. Impact of sulfuric and nitric acids on carbonate dissolution, and the associated deficit of CO_2 uptake in the upper-middle reaches of the Wujiang River, China. J. Contam. Hydrol. 203, 18–27.

Humborg, C., Blomqvist, S., Avsan, E., Bergensund, Y., Smedberg, E., Brink, J., Mörth, C.-M., 2002. Hydrological alterations with river damming in northern Sweden: implications for weathering and river biogeochemistry. Glob. Biogeochem. Cycles 16 (12-11-12-13).

Jia, S., Dai, X., Zhang, D., Dai, L., Wang, R., Zhao, J., 2013. Improved bioproduction of short-chain fatty acids from waste activated sludge by perennial ryegrass addition. Water Res. 47, 4576–4584.

Jiang, G.Y., Zhang, Y.J., Wei, X., Zhang, D.X., Liu, S.L., 2018. The soil infrared spectral characteristics of soil organic matter under different carbon saturation levels. Sci. Agric. Sin. 51, 3117–3129.

Kadnikov, V.V., Savvichev, A.S., Mardanov, A.V., Beletsky, A.V., Merkel, A.Y., Ravin, N.V., Pimenov, N.V., 2019. Microbial communities involved in the methane cycle in the near-bottom water layer and sediments of the meromictic subarctic Lake Svetloe. Antonie Van Leeuwenhoek 112, 1801–1814.

Kanehisa, M., 2004. The KEGG resource for deciphering the genome. Nucleic Acids Res. 32 (277D-280).

Kanehisa, M., Sato, Y., Morishima, K., 2016. BlastKOALA and GhostKOALA: KEGG tools for functional characterization of genome and metagenome sequences. J. Mol. Biol. 428, 726–731.

Knoll, L.B., Vanni, M.J., Renwick, W.H., Kollie, S., 2014. Burial rates and stoichiometry of sedimentary carbon, nitrogen and phosphorus in Midwestern US reservoirs. Freshw. Biol. 59, 2342–2353.

Kozich, J.J., Westcott, S.L., Baxter, N.T., Highlander, S.K., Schloss, P.D., 2013. Development of a dual-index sequencing strategy and curation pipeline for analyzing amplicon sequence data on the MiSeq Illumina sequencing platform. Appl. Environ. Microbiol. 79, 5112–5120.

Langmead, B., Salzberg, S.L., 2012. Fast gapped-read alignment with Bowtie 2. Nat. Methods 9, 357–359.

Lehner, B., Liermann, C.R., Revenga, C., Vörösmarty, C., Fekete, B., Crouzet, P., Döll, P., Endejan, M., Frenken, K., Magome, J., Nilsson, C., Robertson, J.C., Rödel, R., Sindorf, N., Wisser, D., 2011. High-resolution mapping of the world's reservoirs and dams for sustainable river-flow management. Front. Ecol. Environ. 9, 494–502.

Letunic, Ivica, Bork, Peer, 2016. Interactive tree of life (iTOL) v3: an online tool for the display and annotation of phylogenetic and other trees. Nucleic Acids Res. 290, 1–4.

Lever, M.A., Teske, A.P., 2015. Diversity of methane-cycling archaea in hydrothermal sediment investigated by general and group-specific PCR primers. Appl. Environ. Microbiol. 81, 1426–1441.

Li, C., Ji, H., 2016. Chemical weathering and the role of sulfuric and nitric acids in carbonate weathering: isotopes (^{13}C, ^{15}N, ^{34}S, and ^{18}O) and chemical constraints. J. Geophys. Res. Biogeosci. 121, 1288–1305.

Li, S., Zhang, Q., 2014. Carbon emission from global hydroelectric reservoirs revisited. Environ. Sci. Pollut. Res. Int. 21, 13636–13641.

Liang, B., Wang, L.Y., Mbadinga, S.M., Liu, J.F., Yang, S.Z., Gu, J.D., Mu, B.Z., 2015. Anaerolineaceae and Methanosaeta turned to be the dominant microorganisms in alkanes-dependent methanogenic culture after long-term of incubation. AMB Express 5, 1–13.

Liu, X.L., Li, S.L., Wang, Z.L., Wang, B.L., Han, G.L., Wang, F.S., Bai, L., Xiao, M., Yue, F.J., Liu, C.Q., 2018a. Sources and key processes controlling particulate organic nitrogen in impounded river–reservoir systems on the Maotiao River, southwest China. Inland Waters 8, 167–175.

Liu, Z., Sun, Y., Zhang, Y., Feng, W., Lai, Z., Fa, K., Qin, S., 2018b. Metagenomic and 13C tracing evidence for autotrophic atmospheric carbon absorption in a semiarid desert. Soil Biol. Biochem. 125, 156–166.

Liu, L., Yang, Z., Delwiche, K.B., Long, L., Lorke, A., 2020. Spatial and temporal variability of methane emissions from cascading reservoirs in the Upper Mekong River. Water Res. 186, 116319–116330.

Lyautey, E., Billard, E., Tissot, N., Jacquet, S., Domaizon, I., 2021. Seasonal dynamics of abundance, structure, and diversity of methanogens and methanotrophs in lake sediments. Microb. Ecol. 10, 248–261.

Maavara, T., Parsons, C.T., Ridenour, C., Stojanovic, S., Durr, H.H., Powley, H.R., Van Cappellen, P., 2015. Global phosphorus retention by river damming. PNAS 112, 15603–15608.

Meyers, P.A., 1994. Preservation of elemental and isotopic source identification of sedimentary organic matter. Chem. Geol. 114, 289–302.

Meyers, P.A., Ishiwatari, R., 1993. Lacustrine organic geochemistry—an overview of indicators of organic matter sources and diagenesis in lake sediments. Org. Geochem. 20, 867–900.

Moodley, L., Middelburg, J.J., Soetaert, K., Boschker, H.T.S., Herman, P.M.J., Heip, C.H.R., 2005. Similar rapid response to phytodetritus deposition in shallow and deep-sea sediments. J. Mar. Res. 63, 457–469.

Nobu, M.K., Narihiro, T., Hideyuki, T., Qiu, Y.L., Sekiguchi, Y., Woyke, T., Goodwin, L., Davenport, K.W., Kamagata, Y., Liu, W.T., 2015. The genome of Syntrophorhabdus aromaticivorans strain UI provides new insights for syntrophic aromatic compound metabolism and electron flow. Environ. Microbiol. 17, 4861–4872.

Nobu, M.K., Narihiro, T., Kuroda, K., Mei, R., Liu, W.T., 2016. Chasing the elusive Euryarchaeota class WSA2: genomes reveal a uniquely fastidious methyl-reducing methanogen. ISME J. 10, 2478–2487.

Nurk, S., Meleshko, D., Korobeynikov, A., Pevzner, P.A., 2017. metaSPAdes: a new versatile metagenomic assembler. Genome Res. 27, 824–834.

Oremland, R.S., Marsh, L.M., Polcin, S., 1982. Methane production and simultaneous sulphate reduction in anoxic, salt marsh sediments. Nature. 296, 143–145.

Pan, J., Chen, Y., Wang, Y., Zhou, Z., Li, M., 2019. Vertical distribution of bathyarchaeotal communities in mangrove wetlands suggests distinct niche preference of bathyarchaeota subgroup 6. Microb. Ecol. 77, 417–428.

Parks, D.H., Imelfort, M., Skennerton, C.T., Hugenholtz, P., Tyson, G.W., 2015. CheckM: assessing the quality of microbial genomes recovered from isolates, single cells, and metagenomes. Genome Res. 25, 1043–1055.

Parks, Donovan H., Chuvochina, Maria, Waite, David W., Rinke, Christian, Skarshewski, Adam, 2018. A standardized bacterial taxonomy based on genome phylogeny substantially revises the tree of life. Nat. Biotechnol. 4229, 1–12.

Peng, Y., Leung, H.C.M., Yiu, S.M., Chin, F.Y.L., 2012. IDBA-UD: a de novo assembler for single-cell and metagenomic sequencing data with highly uneven depth. Bioinformatics 28, 1420–1428.

Price, Morgan N., Dehal, Paramvir S., Arkin, Adam P., 2009. FastTree: computing large minimum evolution trees with profiles instead of a distance matrix. Mol. Biol. Evol. 26, 1641–1650.

Pyzik, A., Ciezkowska, M., Krawczyk, P.S., Sobczak, A., Drewniak, L., Dziembowski, A., Lipinski, L., 2018. Comparative analysis of deep sequenced methanogenic communities: identification of microorganisms responsible for methane production. Microb. Cell Factories 17, 11–16.

Robinson, J.A., Tiedje, J.M., 1984. Competition between sulfate-reducing and methanogenic bacteria for H2 under resting and growing conditions. Arch. Microbiol. 137, 26–32.

Rui, J., Li, J., Zhang, S., Yan, X., Wang, Y., Li, X., 2015. The core populations and co-occurrence patterns of prokaryotic communities in household biogas digesters. Biotechnol. Biofuels 8, 158–173.

Saunois, M., Bousquet, P., Poulter, B., Peregon, A., Ciais, P., Canadell, J.G., Dlugokencky, E.J., Etiope, G., Bastviken, D., Houweling, S., Janssens-Maenhout, G., Tubiello, F.N., Castaldi, S., Jackson, R.B., Alexe, M., Arora, V.K., Beerling, D.J., Bergamaschi, P., Blake, D.R., Brailsford, G., Brovkin, V., Bruhwiler, L., Crevoisier, C., Crill, P., Covey, K., Curry, C., Frankenberg, C., Gedney, N., Höglund-Isaksson, L., Ishizawa, M., Ito, A., Joos, F., Kim, H.-S., Kleinen, T., Krummel, P., Lamarque, J.-F., Langenfelds, R., Locatelli, R., Machida, T., Maksyutov, S., McDonald, K.C., Marshall, J., Melton, J.R., Morino, I., Naik, V., O'Doherty, S., Parmentier, F.-J.W., Patra, P.K., Peng, C., Peng, S., Peters, G.P., Pison, I., Prigent, C., Prinn, R., Ramonet, M., Riley, W.J., Saito, M., Santini, M., Schroeder, R., Simpson, I.J., Spahni, R., Steele, P., Takizawa, A., Thornton, B.F., Tian, H., Tohjima, Y., Viovy, N., Voulgarakis, A., van Weele, M., van der Werf, G.R., Weiss, R., Wiedinmyer, C., Wilton, D.J., Wiltshire, A., Worthy, D., Wunch, D., Xu, X., Yoshida, Y., Zhang, B., Zhang, Z., Zhu, Q., 2016. The global methane budget 2000–2012. Earth Syst. Sci. Data 8, 697–751.

Saunois, M., Stavert, A.R., Poulter, B., Bousquet, P., Canadell, J.G., Jackson, R.B., Raymond, P.A., Dlugokencky, E.J., Houweling, S., Patra, P.K., Ciais, P., Arora, V.K., Bastviken, D., Bergamaschi, P., Blake, D.R., Brailsford, G., Bruhwiler, L., Carlson, K.M., Carrol, M., Castaldi, S., Chandra, N., Crevoisier, C., Crill, P.M., Covey, K., Curry, C.L., Etiope, G., Frankenberg, C., Gedney, N., Hegglin, M.I., Höglund-Isaksson, L., Hugelius, G., Ishizawa, M., Ito, A., Janssens-Maenhout, G., Jensen, K.M., Joos, F., Kleinen, T., Krummel, P.B., Langenfelds, R.L., Laruelle, G.G., Liu, L., Machida, T., Maksyutov, S., McDonald, K.C., McNorton, J., Miller, P.A., Melton, J.R., Morino, I., Müller, J., Murguia-Flores, F., Naik, V., Niwa, Y., Noce, S., O'Doherty, S., Parker, R.J., Peng, C., Peng, S., Peters, G.P., Prigent, C., Prinn, R., Ramonet, M., Regnier, P., Riley, W.J., Rosentreter, J.A., Segers, A., Simpson, I.J., Shi, H., Smith, S.J., Steele, L.P., Thornton, B.F., Tian, H., Tohjima, Y., Tubiello, F.N., Tsuruta, A., Viovy, N., Voulgarakis, A., Weber, T.S., van Weele, M., van der Werf, G.R., Weiss, R.F., Worthy, D., Wunch, D., Yin, Y., Yoshida, Y., Zhang, W., Zhang, Z., Zhao, Y., Zheng, B., Zhu, Q., Zhu, Q., Zhuang, Q., 2020. The global methane budget 2000–2017. Earth Syst. Sci. Data 12, 1561–1623.

Schink, B., 1997. Energetics of syntrophic cooperation in methanogenic degradation. Microbiol. Mol. Biol. Rev. 61, 262–280.

Schloss, P.D., Westcott, S.L., Ryabin, T., Hall, J.R., Hartmann, M., Hollister, E.B., Lesniewski, R.A., Oakley, B.B., Parks, D.H., Robinson, C.J., Sahl, J.W., Stres, B., Thallinger, G.G., Van Horn, D.J., Weber, C.F., 2009. Introducing mothur: open-source, platform-independent, community-supported software for describing and comparing microbial communities. Appl. Environ. Microbiol. 75, 7537–7541.

Schnell, S., Ratering, S., Jansen, K., 1998. Simultaneous determination of iron(III), iron(II), and manganese(II) in environmental samples by ion chromatography. Environ. Sci. Technol. 32, 1530–1537.

Sedano-Nunez, V.T., Boeren, S., Stams, A.J.M., Plugge, C.M., 2018. Comparative proteome analysis of propionate degradation by Syntrophobacter fumaroxidans in pure culture and in coculture with methanogens. Environ. Microbiol. 20, 1842–1856.

Segata, N., Bornigen, D., Morgan, X.C., Huttenhower, C., 2013. PhyloPhlAn is a new method for improved phylogenetic and taxonomic placement of microbes. Nat. Commun. 4, 2304–2314.

Sepulveda-Jauregui, A., Hoyos-Santillan, J., Martinez-Cruz, K., Walter Anthony, K.M., Casper, P., Belmonte-Izquierdo, Y., Thalasso, F., 2018. Eutrophication exacerbates the impact of climate warming on lake methane emission. Sci. Total Environ. 636, 411–419.

Shi, W., Chen, Q., Yi, Q., Yu, J., Ji, Y., Hu, L., Chen, Y., 2017. Carbon emission from cascade reservoirs: spatial heterogeneity and mechanisms. Environ. Sci. Technol. 51, 12175–12181.

Syvitski, J.P., Vorosmarty, C.J., Kettner, A.J., Green, P., 2005. Impact of humans on the flux of terrestrial sediment to the global coastal ocean. Science 308, 376–380.

Tesi, T., Semiletov, I., Dudarev, O., Andersson, A., Gustafsson, Ö., 2016. Matrix association effects on hydrodynamic sorting and degradation of terrestrial organic matter during cross-shelf transport in the Laptev and East Siberian shelf seas. J. Geophys. Res. Biogeosci. 121, 731–752.

Thauer, R.K., Kaster, A.-K., Seedorf, H., Buckel, W., Hedderich, R., 2008. Methanogenic archaea: ecologically relevant differences in energy conservation. Nat. Rev. Microbiol. 6, 579–591.

Wang, F., Wang, B., Liu, C.-Q., Wang, Y., Guan, J., Liu, X., Yu, Y., 2011. Carbon dioxide emission from surface water in cascade reservoirs–river system on the Maotiao River, southwest of China. Atmos. Environ. 45, 3827–3834.

Wang, B., Liu, C.-Q., Peng, X., Wang, F., 2013. Mechanisms controlling the carbon stable isotope composition of phytoplankton in karst reservoirs. J. Limnol. 72, 127–139.
Wang, Maberly, S.C., Wang, B., Liang, X., 2018a. Effects of dams on riverine biogeochemical cycling and ecology. Inland Waters 8, 130–140.
Wang, Qiu, X.-L., Peng, X., Wang, F., 2018b. Phytoplankton community structure and succession in karst cascade reservoirs, SW China. Inland Waters 8, 229–238.
Wang, B., Zhang, H., Liang, X., Li, X., Wang, F., 2019. Cumulative effects of cascade dams on river water cycle: evidence from hydrogen and oxygen isotopes. J. Hydrol. 568, 604–610.
Wang, W., Yi, Y., Zhong, J., Kumar, A., Li, S.-L., 2020a. Carbon biogeochemical processes in a subtropical karst river–reservoir system. J. Hydrol. 591, 591–601.
Wang, W.F., Li, S.L., Zhong, J., Maberly, S.C., Li, C., Wang, F.S., Xiao, H.Y., Liu, C.Q., 2020b. Climatic and anthropogenic regulation of carbon transport and transformation in a karst river-reservoir system. Sci. Total Environ. 707, 135628–135638.
Wawrik, B., Marks, C.R., Davidova, I.A., McInerney, M.J., Pruitt, S., Duncan, K.E., Suflita, J.M., Callaghan, A.V., 2016. Methanogenic paraffin degradation proceeds via alkane addition to fumarate by 'Smithella' spp. mediated by a syntrophic coupling with hydrogenotrophic methanogens. Environ. Microbiol. 18, 2604–2619.
Wei, B., Mollenhauer, G., Hefter, J., Grotheer, H., Jia, G., 2020. Dispersal and aging of terrigenous organic matter in the Pearl River Estuary and the northern South China Sea Shelf. Geochim. Cosmochim. Acta 282, 324–339.
Whiticar, M.J., Faber, E., Schoell, M., 1986. Biogenic methane formation in marine and freshwater environments: CO_2 reduction vs. acetate fermentation—isotope evidence. Geochim. Cosmochim. Acta 50, 693–709.
Worm, P., Koehorst, J.J., Visser, M., Sedano-Núñez, V.T., Schaap, P.J., Plugge, C.M., Sousa, D.Z., Stams, A.J.M., 2014. A genomic view on syntrophic versus non-syntrophic lifestyle in anaerobic fatty acid degrading communities. Biochim. Biophys. Acta Bioenerg. 1837, 2005–2015.
Xiao, J., Wang, B., Qiu, X.L., Yang, M., Liu, C.Q., 2021. Interaction between carbon cycling and phytoplankton community succession in hydropower reservoirs: evidence from stable carbon isotope analysis. Sci. Total Environ. 774, 145141–145151.
Yamada, T., Imachi, H., Ohashi, A., Harada, H., Hanada, S., Kamagata, Y., Sekiguchi, Y., 2007. Bellilinea caldifistulae gen. nov., sp. nov. and Longilinea arvoryzae gen. nov., sp. nov., strictly anaerobic, filamentous bacteria of the phylum Chloroflexi isolated from methanogenic propionate-degrading consortia. Int. J. Syst. Evol. Microbiol. 57, 2299–2306.
Yongkyu, K., Werner, L., Ahmed, M., 2015. Differential assemblage of functional units in paddy soil microbiomes. PLoS One 10, 1–20.
Youngblut, N.D., Dell'aringa, M., Whitaker, R.J., 2014. Differentiation between sediment and hypolimnion methanogen communities in humic lakes. Environ. Microbiol. 16, 1411–1423.
Yuan, Q., Hernández, M., Dumont, M.G., Rui, J., Fernández Scavino, A., Conrad, R., 2018. Soil bacterial community mediates the effect of plant material on methanogenic decomposition of soil organic matter. Soil Biol. Biochem. 116, 99–109.
Zhang, C.J., Pan, J., Liu, Y., Duan, C.H., Li, M., 2020. Genomic and transcriptomic insights into methanogenesis potential of novel methanogens from mangrove sediments. Microbiome 8, 94–106.
Zhao, Y., Liu, P., Rui, J., Cheng, L., Wang, Q., Liu, X., Yuan, Q., 2020a. Dark carbon fixation and chemolithotrophic microbial community in surface sediments of the cascade reservoirs, Southwest China. Sci. Total Environ. 698, 134316–134325.
Zhao, Z., Li, S., Xue, L., Liao, J., Zhao, J., Wu, M., Wang, M., Sun, J., Zheng, Y., Yang, Q., 2020b. Effects of dam construction on arsenic mobility and transport in two large rivers in Tibet, China. Sci. Total Environ. 741, 140406–140417.
Zheng, H., Zhao, X., Zhao, T., Chen, F., Xu, W., Duan, X., Wang, X., Ouyang, Z., 2011. Spatial-temporal variations of methane emissions from the Ertan hydroelectric reservoir in southwest China. Hydrol. Process. 25, 1391–1396.
Zhuang, G.C., Elling, F.J., Nigro, L.M., Samarkin, V., Joye, S.B., Teske, A., Hinrichs, K.U., 2016. Multiple evidence for methylotrophic methanogenesis as the dominant methanogenic pathway in hypersaline sediments from the Orca Basin, Gulf of Mexico. Geochim. Cosmochim. Acta 1–20.
Zhuang, G.-C., Heuer, V.B., Lazar, C.S., Goldhammer, T., Wendt, J., Samarkin, V.A., Elvert, M., Teske, A.P., Joye, S.B., Hinrichs, K.-U., 2018. Relative importance of methylotrophic methanogenesis in sediments of the Western Mediterranean Sea. Geochim. Cosmochim. Acta 224, 171–186.